Available online at www.sciencedirect.com
SCIENCE DIRECT
Polymer 47 (2006) 4251–4260
polymer
www.elsevier.com/locate/polymer

Synthesis and characterization of two shape-memory polymers containing short aramid hard segments and poly(ε-caprolactone) soft segments

Gouher Rabani [a], Heinrich Luftmann [b], Arno Kraft [a,*]

[a] *Chemistry, School of Engineering and Physical Sciences, Heriot-Watt University, Riccarton, Edinburgh EH14 4AS, UK*
[b] *Organisch-Chemisches Institut der Universität Münster, Abteilung Massenspektrometrie, Corrensstraße 40, D-48149 Münster, Germany*

Received 22 November 2005; received in revised form 27 March 2006; accepted 30 March 2006
Available online 2 May 2006

Abstract

A number of segmented copolymers were synthesized by reacting 4-aminobenzoyl end-functionalized poly(ε-caprolactone)s of M_n 2000, 3000 and 4000 g mol^{-1} with three aromatic diacid dichlorides in the presence of chlorotrimethylsilane. Polymer purity, molar mass, thermal and mechanical properties were characterized by NMR, MALDI-TOF mass spectrometry, GPC, DSC, and DMTA. Promising shape-memory properties were observed for two polymers that contained comparatively short, semicrystalline poly(ε-caprolactone) soft segments of molecular weight 3000 g mol^{-1} and either terephthalamide or 2,6-naphthalenedicarboxyamide hard segments. Cast films of these polymers were soft and elastomer-like at room temperature. Loading could be conveniently achieved by cold-drawing at room temperature and strain recovery took place upon heating above the melting temperature of the soft segment (35 °C). Cast films reached uniform deformation properties with strain recovery rates as high as 99% and strain fixity values of 78% after passing through only one or two training cycles.

Keywords: Aramid; Elastomer; Poly(ε-caprolactone)

1. Introduction

A shape-memory material has the ability to remember its permanent shape after being deformed into a temporary shape, whereby the temporary shape remains stable even after the stress responsible for the deformation is released. An external stimulus—most commonly a change in temperature and, more rarely, irradiation or a change in pH—is required for a deformed shape-memory material to recover its original stress-free state, the driving force being the elastic energy stored during the initial deformation. Shape-memory alloys, such as nickel–titanium alloy (Nitinol®), have been studied extensively for over 40 years, and they are now utilized in a variety of applications including flexible eye-glass frames, self-adjusting orthodontic wires, stents, actuators, and temperature-responsive valves [1–3]. However, high manufacture costs have so far restricted the use of these materials to specialized areas where performance requirements outweigh the high price.

Certain polymers, too, show shape-memory behavior, and they promise to provide a cheaper alternative due to their ease of preparation and processing [4]. Moreover, whereas the shape recovery in alloys is enthalpy-driven, it is an entropy-driven process in polymers. Almost all shape-memory polymers (SMPs) are rubber-elastic to a certain extent, which allows for much greater deformations up to several 100% in certain cases. Like elastomers, SMPs have to be either covalently or physically cross-linked. Polymer networks are less susceptible to creep, thus ensuring excellent reproducibility of the shape-memory transition even after many cycles [5–8]. However, if solution or melt processibility and recyclability is desired, an SMP needs to be a thermoplastic.

The most prominent thermoplastic SMPs are polyurethanes [4]. Structurally, they consist of suitably chosen polyester or polyether soft segments and oligourethane hard segments that alternate along the polymer chain. The soft segment is responsible for a thermal shape-memory effect that occurs when the polymer is heated above the shape-memory transition temperature T_s. Soft segments are glassy or semi-crystalline below T_s. The purpose of the hard segments is to fix the permanent shape through physical cross-links, which must, therefore, be thermally stable well above T_s. A wide range of switching temperatures T_s between −50 and +70 °C has been

* Corresponding author. Tel.: +44 131 4518040; fax: +44 131 4513180.
E-mail address: a.kraft@hw.ac.uk (A. Kraft).

0032-3861/$ - see front matter © 2006 Elsevier Ltd. All rights reserved.
doi:10.1016/j.polymer.2006.03.106

reported, and T_s can be varied by the choice of soft and hard segment [4].

Polyurethane-based SMPs are easily processed by conventional techniques (e.g. extrusion or casting) and they are among the more promising low-cost, low-density materials with excellent shape-memory ability and flexibility. The first polyurethanes with shape-memory properties were introduced on the market by Mitsubishi in the early 1990s [9,10]. However, only selected data are available that quantify their shape-memory properties [11]. The exact composition of these SMPs has not been published, but they seem to consist of a relatively complex combination of short amorphous polyester and polyether soft segments, short diol chain extenders, and aromatic urethane hard segments. Surprisingly, few commercial applications have so far emerged. Examples are components in auto-chokes, adjustable spoon and fork handles for handicapped, and water-permeable membranes in upmarket active-wear [11].

Although shape-memory polymers with amorphous soft segments have the advantage that they are able to store, in principle, more elastic energy, the adjustment of the T_g to a certain temperature is not straightforward and usually requires the judicious combination of several different soft segments [9,10,12–14]. A less complicated alternative is to choose a soft segment that crystallizes below T_s. In the mid-1990s, Kim and co-workers reported structurally simple and well-defined segmented polyurethanes with poly(ε-caprolactone) (PCL) soft segments that showed excellent shape-memory properties [15,16]. These SMPs were obtained from poly(ε-caprolactone) telechelics of varying lengths (M_n 2000–8000 g mol^{-1}), 4,4′-methylenebis(phenyl isocyanate), and 1,4-butanediol, using a pre-polymer method common to many polyurethane syntheses. Kim's polymers had switching temperatures between 44 and 55 °C depending on the molecular weight of the soft segment. The crystallinity of the PCL segments increased with increasing M_n, whereas polymers made from a PCL with an M_n of only 2000 g mol^{-1} were unsuitable because they failed to crystallize. The optimum hard segment content was 30–45 wt%, whereas below 10 wt% the hard domains were unable to provide the required physical cross-links and led to insufficient mechanical strength. The best shape-memory properties were obtained for polymers containing (a) long PCL segments (M_n 4000 or 8000 g mol^{-1}) and (b) a high fraction (30–45 wt%) of hard segments. Strain recovery rates approached 98% in these cases provided that the applied strain was kept low.

More recently, Lendlein and Langer developed PCL-based, biodegradable SMPs that possessed some of the best shape-memory properties reported so far [17]. These polymers are currently explored for surgical sutures and other biomedical applications. They were made from a poly(ε-caprolactone)-diol of unspecified M_n, an aliphatic diisocyanate and a poly(*p*-dioxanone)-diol. Again, a high hard segment concentration was crucial, as the semicrystalline poly(dioxanone) segments—and probably also the oligourethane units—contributed to the hard segment in these SMPs.

Until now, the majority of literature-reported non-cross-linked SMPs have urethane hard segments. It is well known that polyurethanes tend to degrade upon heating to or above the melting temperature, which hampers their melt processing. As Gaymans and co-workers have demonstrated in a series of papers, there are considerable advantages in replacing urethanes by aromatic amide (aramid) units. Uniform aramid hard segments are fast-crystallizing [18,19], induce high fracture strain and toughness, and show excellent phase separation and thermal stability [20,21]. This generally leads to a significant improvement in mechanical and thermal properties over related polyurethane elastomers containing the same soft segment.

We describe here the first examples of SMPs that contain aramid hard segments and comparatively short poly(ε-caprolactone) soft segments. The synthesis of these polymers made use of a recently reported mild low-temperature polymerization route, which avoided not only high temperatures but also toxic isocyanates as well as carcinogenic aromatic amines [22,23]. Shape-memory polymers with short aramid hard segments turned out to be far easier to manipulate below T_s than their polyurethane-based counterparts. The new SMPs could be stretched at room temperature and fixed into their temporary shape by a simple cold-drawing process, while recovery of the original shape took place upon heating to 55 °C. This paper outlines the influence of variations of the hard and soft segments on the properties, both thermal and mechanical, of such aramid-based SMPs.

2. Experimental

2.1. Materials

Terephthaloyl chloride (**M1**), triethylamine, chlorotrimethylsilane, 4-nitrobenzoyl chloride, and anhydrous *N*,*N*-dimethylacetamide were supplied by Lancaster or Aldrich. Toluene and methanol were purchased from Fisher Chemicals, and acetic acid from Fisons. Poly(ε-caprolactone)-diols CAPA 2200P, CAPA 2302A, and CAPA 2402 with M_n values of 2000, 3000, and 4000 g mol^{-1}, respectively, were provided by Solvay Caprolactones. All materials were used as received without further purification. 2,6-Naphthalenedicarbonyl dichloride (**M2**) and 4,4′-biphenyldicarbonyl dichloride (**M3**) were synthesized as reported previously [22]. The synthesis and characterization of telechelic **T1** (derived from PCL 2000) was described in an earlier paper [24] (Fig. 1).

2.2. Synthetic procedures

2.2.1. Poly(ε-caprolactone) α,ω-bis(4-aminobenzoate) (*T2*)

Triethylamine (10 mL, 75 mmol) was added to a solution of poly(ε-caprolactone)-diol (M_n 3000 g mol^{-1}, 96.0 g, 32.0 mmol) in toluene (200 mL). The solution was left for 10 min, then heated to 50 °C before a solution of 4-nitrobenzoyl chloride (13.0 g, 70.0 mmol) in toluene (300 mL) was added dropwise over 30 min. The mixture was then refluxed for 4 days. After cooling to room temperature, the precipitate (triethylammonium chloride) was removed by suction filtration. The filtrate was washed with 5% aqueous $NaHCO_3$

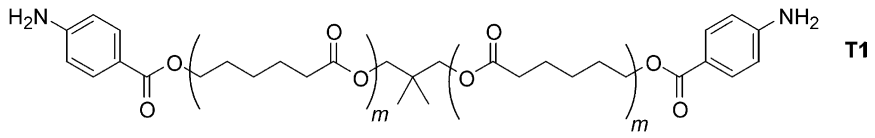

Fig. 1. Structure of telechelic **T1**.

(500 mL). The organic phase was separated and concentrated on a rotary evaporator. Drying in vacuum (120 °C/0.2 mbar) gave an orange, waxy solid. Yield: 97.0 g (92%). ^{1}H NMR (200 MHz, $CDCl_3$): δ 1.21–1.85 (m, ca. 156H), 2.27 (~t, ca. 50H, CH_2CO), 4.01 (t, J=6.6 Hz, ca. 50H, CH_2O), 4.33 (t, J=6.6 Hz, 4H, $ArCO_2CH_2$), 8.16 and 8.25 ($AA'BB'$, 2×4H, ArH).

A mixture of iron powder (22.5 g, 403 mmol), toluene (500 mL), water (60 mL), and acetic acid (2 mL) was refluxed for 1 h until an emulsion had formed. A solution of the nitrobenzoyl end-capped poly(ε-caprolactone) (97 g, ca. 29 mmol) in toluene (60 mL) was then added dropwise over 30 min, and refluxing was continued for 2 days. The hot mixture was filtered, and the filtrate was washed with water (2×500 mL). The toluene phase was separated and concentrated on a rotary evaporator. The brown, waxy **T2** was then dried in vacuum (120 °C/0.2 mbar) until toluene could no longer be detected in the ^{1}H NMR spectrum. Yield: 85.0 g (89%). ^{1}H NMR (200 MHz, $CDCl_3$): δ 1.26–1.45 (m, ca. 50H), 1.45–1.80 (m, ca. 106H), 2.28 (~t, ca. 50H, CH_2CO), 4.03 (t, J=6.6 Hz, ca. 50H, CH_2O), 4.12 (brs, 4H, NH_2), 4.23 (t, J=6.6 Hz, 4H, $ArCO_2CH_2$), 6.61 and 7.81 ($AA'XX'$, 2×4H, ArH).

2.2.2. Typical polymerization procedure

Chlorotrimethylsilane (0.46 mL, 3.6 mmol) was added to an ice-cold solution of **T2** (4.00 g, 1.21 mmol) in dry DMAc (20 mL). After stirring for 15 min, a solution of terephthaloyl chloride (0.246 g, 1.21 mmol) in dry DMAc (10 ml) was added dropwise with a gastight syringe. The polymerization mixture became viscous within 15 min, and stirring at 20 °C was continued for 18 h. The polymer was precipitated into methanol, collected by suction filtration, and dried in vacuum (100 °C/0.2 mbar) to give **SMP4** as a colorless solid. Yield: 3.78 g (91%).

2.3. NMR

^{1}H NMR spectra were recorded on a Bruker AC 200.

2.4. IR

Infrared spectra were recorded with a Perkin–Elmer RX Fourier transform infrared spectrometer. Films were cast from DMAc solution onto NaCl plates, followed by slow evaporation of the solvent at 80 °C for 2 days in an oven.

2.5. MALDI-TOF MS

Matrix-assisted laser desorption ionization time-of-flight (MALDI-TOF) mass spectra were recorded in linear or reflectron mode on a Bruker Daltonics (Bremen) Reflex IV instrument equipped with a 337 nm nitrogen laser. The resolution, FWHM, was ca. 20,000 under optimal conditions. Calibration with poly(ethylene glycol) ($M+Na^+$ ion peaks) in the m/z range of 600–4000 gave a mass accuracy of $\pm$0.02%. Samples were prepared by combining chloroform solutions of the telechelic (50 μL) and 2,5-dihydroxybenzoic acid (50 μL, at a concentration of ca. 50 mg/mL) with saturated methanolic $NaBF_4$ (10 μL) in a ratio of approximately 50:1:2 (w/w/w, matrix/polymer/$NaBF_4$). A 1 μL sample of this mixture was dropped onto the target, the solvent was allowed to evaporate, and mass spectra were averaged over 50–200 laser shots (pulse length 3 ns) distributed over different parts of the target.

2.6. GPC

Molecular weight distributions were determined by gel-permeation chromatography (GPC) using a Waters 590 programmable HPLC pump equipped with a Waters 410 differential refractometer and two Polymer Laboratories 5 μm mixed-C columns (calibrated with polystyrene standards; elution solvent: THF; flow rate: 1.0 mL min^{-1}; temperature: 35 °C).

2.7. DSC

Samples were analyzed with a Thermal Advantage DSC 2010 at a heating rate of 20 K min^{-1} under a constant nitrogen flow. Samples were cut from cast films prepared in the same manner as for tensile testing. Glass transitions were taken as the mid-point of the inflexion.

2.8. DMTA

Dynamic mechanical analysis measurements were carried out in tensile mode with a TA Instruments DMA 2980 at a frequency of 3 Hz and a heating rate of 2 °C min^{-1}. Samples were prepared as for DSC and tensile testing by casting a viscous solution of the polymer (ca. 0.6 g) in DMAc (4 mL) onto Teflon plates, followed by slow evaporation of the solvent in an oven at 80 °C for 2 days. ^{1}H NMR spectra confirmed that the as-prepared polymer films were free of solvent.

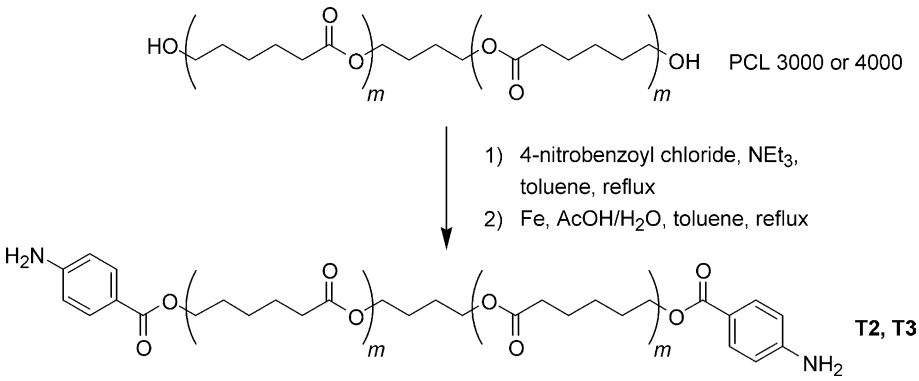

Fig. 2. Reaction scheme for the modification of the poly(ε-caprolactone)-diol precursors.

2.9. Tensile tests and shape-memory effect

Tensile and cyclic thermomechanical tests were carried out with an Instron Model 1026 tensile tester. A heating chamber was constructed from aluminium foil and two thermostatically controlled convection heaters. Cyclic tests were performed by straining a sample to 200, 300, or 400% (ε_m) at a speed of 50 mm min^{-1}. The speed was then reversed, and the sample was allowed to relax freely at room temperature (19 °C) until a constant strain ε_u was reached. The sample was then heated to 55 °C (with convection heaters set to this temperature) for 15 min. The residual strain ε_p after recovery was recorded and completed one full test cycle (Fig. 10).

The shape-memory properties were quantified using the various strain values obtained in the cyclic experiment [4]. Eq. (1) defines the strain recovery rate (R_r) as a measure of how much of the strain, which has been applied in the programming stage, is recovered during the shape-memory transition from one cycle to the next

$$R_r(N) = \frac{\varepsilon_m - \varepsilon_p(N)}{\varepsilon_m - \varepsilon_p(N-1)} \quad (1)$$

where N is the cycle number. The percentage strain recovery (Eq. (2)) is the amount of the applied strain that is recovered in the same cycle following heating above T_s.

$$\%\ \text{Strain recovery} = \frac{\varepsilon_m - \varepsilon_p}{\varepsilon_m} \times 100\% \quad (2)$$

Finally, the percentage strain fixity (Eq. (3)) quantifies the ability of the switching segment to hold the shape after the sample has been stretched.

$$\%\ \text{Strain fixity} = \frac{\varepsilon_u}{\varepsilon_m} \times 100\% \quad (3)$$

3. Results and discussion

3.1. Synthesis of telechelic precursors

Our chosen method of polymerization required that the commercial poly(ε-caprolactone)-diols (PCLs) were functionalized with α,ω-aminobenzoate end groups, following a previously reported procedure (Fig. 2) [22]. The resulting modified telechelics **T1** (from PCL 2000), **T2** (from PCL 3000), and **T3** (from PCL 4000) were thoroughly dried and then analyzed by ^{1}H NMR spectroscopy and MALDI-TOF mass spectrometry. The latter was particularly suited to confirm whether or not the prepared batches of **T1–T3** were indeed fully end-functionalized. It was imperative that the modified telechelics were free of monofunctional impurities having unreacted OH termini, as they would handicap the subsequent polymerization [24].

MALDI-TOF mass spectra of the telechelics were obtained in the linear and reflectron modes. In the linear mode, the mass spectra tended to have poor mass resolution but provided instead an overall representation of the molecular weight distribution (Fig. 3(a)). The MALDI-TOF mass spectra were also recorded in reflectron mode. The improved resolution made it easier to detect byproducts and it helped moreover in their identification. Fig. 4 shows the structures of the various telechelics that could be identified in the MALDI-TOF mass spectra. The expansion of the mass spectrum of **T2** in Fig. 3(b) depicts three distinct series of ion peaks, each separated by 114 Da, the mass of a poly(ε-caprolactone) repeat unit. The most intense ion peaks (**A**) could be assigned to the sodium adduct of the α,ω-bis(aminobenzoyl)-substituted **T2**, while a related series (**A***) at 22 Da to lower m/z values belonged to the H^+ adduct of **T2**. The sodium adduct of cyclic poly(ε-caprolactone), a component already present in the commercial poly(ε-caprolactone), gave rise to a third series (**C**) at 14 Da to higher m/z of the main series. There was no evidence of any monosubstituted products.

Close inspection of the MALDI mass spectrum for a similarly prepared batch of **T3** revealed additional ion peaks (**B** and **B***) at 5 Da below the corresponding diester series, which were identified as the Na^+ and H^+ adducts of a mono-aminobenzoate ester (Fig. 3(c)). The presence of a monofunctional impurity was further evident when two polymerizations, using the same batch of **T3**, turned out to give disappointingly low molar mass products. The preparation of **T3**, therefore, had to be repeated, this time with extended reaction times to take the lower reactivity of the higher-molar-mass telechelic into account and ensure full ester-end-functionalization of the OH end groups.

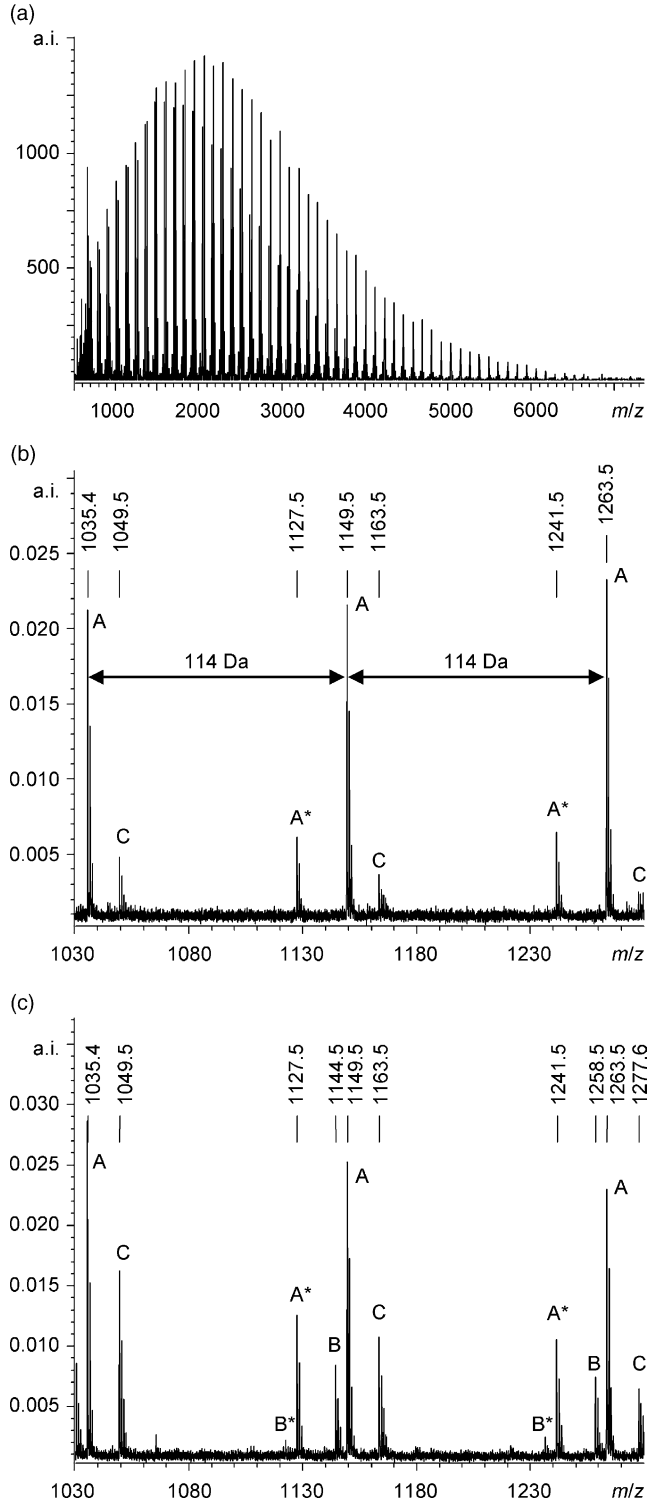

Fig. 3. (a) MALDI-TOF mass spectrum of telechelic **T2** (linear mode, a.i. = arbitrary intensity). (b) Partial spectrum from *m/z* 1030 to 1280 (reflectron mode). (c) Corresponding enlarged detail of the MALDI-TOF mass spectrum (reflectron mode) of telechelic **T3**, which reveals the presence of a monoester impurity (**B**, **B***).

3.2. Polymerization

A series of seven polymers was made from the aromatic diacid dichlorides **M1**–**M3** (shown in Fig. 5) and aminobenzoyl-terminated PCLs **T1**–**T3** (Fig. 6). The condensation polymerization was an adaption of an aramid polymer synthesis by Imai in which the aromatic amine component was activated with chlorotrimethylsilane [25]. Although the reaction is sensitive against moisture, problems with hydrolysis are conveniently prevented by making the *N*-silylated intermediates in situ and by using an excess of $ClSiMe_3$ [26]. Polymer formation was confirmed by a rapid increase in viscosity, as well as by ^1H NMR and GPC (THF, polystyrene standards). The polymers possessed typical weight-average molar masses M_w between 53 and 104 kg mol^{-1}, which were considerably higher than for the only previously reported example of a related polymer obtained by transesterification of an aromatic diamide–diester with PCL 2000 [27].

3.3. Thermal properties: DSC

All polymers showed several distinct transitions in their DSC scans typical of a multi-phase system (Table 1). The amorphous parts of PCL soft segments gave rise to a T_g at about −55 °C. Since, parts of the soft segments were crystalline as well, two melting transitions were observed, one for crystalline PCL soft segments (T_{ms}) at 14–54 °C, and the other for crystalline aramid hard segments (T_{mh}) between 76 and 192 °C. The increase in soft segment length from PCL 2000 to PCL 3000 and finally PCL 4000 had comparatively little effect on T_g, but led to a noticeable increase in the melting temperature T_{ms} of the soft segment and, at the same time, caused a drop in the melting temperature T_{mh} of the hard segments. An increase in T_{ms} within the series **SMP1** (25 °C) < **SMP4** (35 °C) < **SMP7** (54 °C) coincided with a rise in crystallinity of the soft segment as the molar mass of the soft segment became larger [18]. The concomitant decrease in T_{mh} was attributed to the hard segment domains becoming more diluted and dispersed throughout a dominating soft segment matrix.

The choice of hard segment affected T_{mh}, but hardly T_g or T_{ms}. Most notably, 2,6-naphthalenedicarboxamide-containing polymers **SMP2** and **SMP5** gave rise to higher melting temperatures than their counterparts with terephthalamide units in the hard segment [22].

3.4. Hydrogen-bonding: IR spectra

Hydrogen bonding interactions in selected polymer films were studied by infrared spectroscopy, after annealing under conditions similar to those used to make the tensile test samples. Fig. 7(a) shows the NH stretch region of several polymers. The two polymers with 2,6-naphthalenedicarboxamide-based hard segments, **SMP2** and **SMP5**, had relatively sharp NH stretches around 3368 cm^{-1}, indicative of better phase separation, while the NH stretches of **SMP1** and **SMP4**, which both contained terephthalamide hard segments, were much broader.

The C=O stretch region, shown in Fig. 7(b), was dominated by the poly(ε-caprolactone) ester carbonyl stretch (1734 cm^{-1}). A hydrogen-bonded aromatic ester C=O (1698 cm^{-1}) and a non-hydrogen-bonded aromatic amide C=O stretch

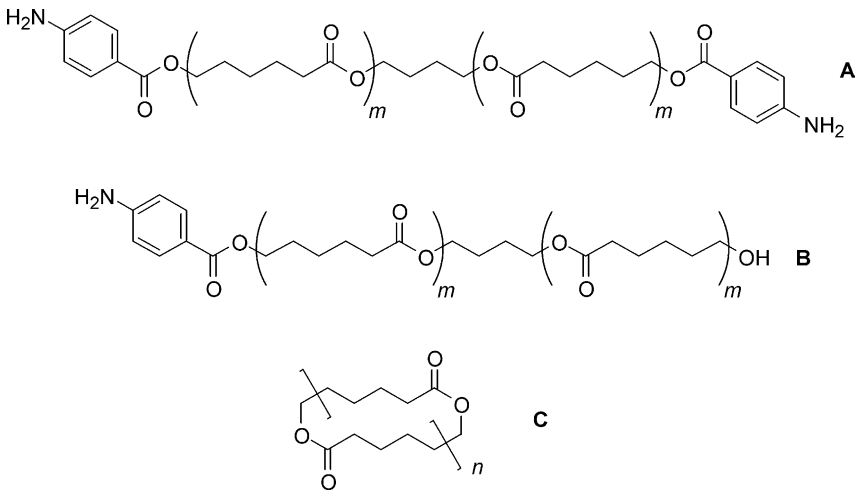

Fig. 4. Structures of the telechelic diamine **A**, monoester impurity **B** and cyclic poly(ε-caprolactone) **C** observed in the MALDI-TOF mass spectra of telechelics **T2** and **T3**.

(1668 cm^{-1}) were clearly evident for **SMP2** and **SMP5**. The IR frequencies suggested that hydrogen bonds formed between amide NH and aromatic ester C=O groups in these two polymers [22,28]. On the contrary, the amide C=O stretches of **SMP1** and **SMP4** were shifted towards 1654 cm^{-1} from which we conclude that the amide C=O groups in these polymers were instead involved in hydrogen-bonding to nearby amide NH groups [19]. In consequence, the aromatic ester was no longer hydrogen-bonded, and its C=O stretch (expected at about 1714 cm^{-1}) [22] could be observed as a shoulder of the aliphatic ester carbonyl peak.

3.5. Thermal properties: DMTA

Dynamic mechanical analysis was a key technique for screening our series of polymers for useful shape-memory properties. The storage modulus as a function of temperature is plotted in Fig. 8. In all cases, the modulus decreased steadily above the T_g of the PCL soft segment, with a noticeable drop occurring at around T_{ms}. It then reached a more or less extended rubbery plateau that is characteristic for thermoplastic elastomers and high-molar-mass thermoplastics.

Fig. 8(a) compares the storage moduli of polymers **SMP1**, **SMP4**, and **SMP7**, which all contain the same terephthalamide hard segment but possess different soft segment lengths (derived from PCL 2000, PCL 3000, and PCL 4000, respectively). Not surprisingly, a longer soft segment lowered the rubbery modulus of the three polymers at around 60 °C resulting from solvation of the hard segment crystallites by the long amorphous soft segments [29]. The coinciding rise in the shape-recovery temperature T_s was largely a consequence of the higher crystallinity of the longer PCL soft segments.

For a good shape-memory material, a large drop in the storage modulus around T_s is crucial. Whereas the glass (E_g) to rubber (E_r) elasticity ratio (E_g/E_r) is often quoted to estimate the magnitude of the change in modulus as the sample undergoes shape recovery [16], we opted instead for looking at the change in modulus between room temperature (19 °C, E'_c), when the soft segment is partially crystalline, and 55 °C (E'_r) just above the onset of the rubbery region. These moduli have the advantage of being more representative of the tensile test conditions used later on. The elasticity ratio is, therefore, defined in this paper as E'_c/E'_r. It increased with the soft segment content (Table 1). When compared to **SMP1**, the higher elasticity ratio for polymer **SMP4** implies a larger

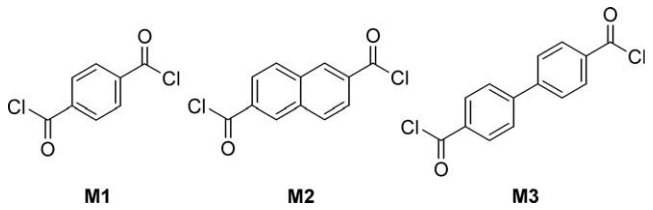

Fig. 5. Structures of diacid dichlorides **M1**–**M3**.

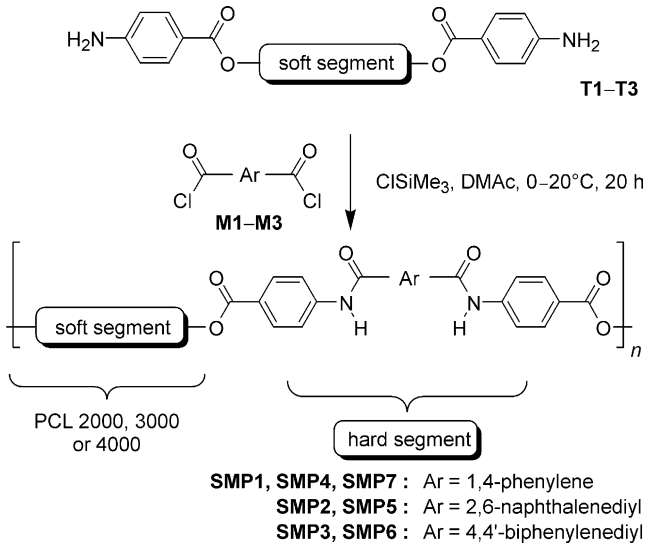

Fig. 6. Reaction scheme for the polymerization.

Table 1
Characteristic data for polymers **SMP1–SMP7**

Polymer	Monomers	M_w[a] (kg mol^{-1})	M_w/M_n[a]	T_g (°C)[b]	T_{ms} (°C)[b]	T_{mh} (°C)[b]	E'_c/E'_r[c]	Hard segment content (%)
SMP1	PCL 2000+**M1**	60	1.3	−53	25	154	2.2	19
SMP2	PCL 2000+**M2**	55	1.4	−55	14	192	1.4	21
SMP3	PCL 2000+**M3**	53	1.5	−53	19	113	2.2	22
SMP4	PCL 3000+**M1**	93	1.4	−55	35	93	15	12
SMP5	PCL 3000+**M2**	89	1.4	−55	27	158	5.4	14
SMP6	PCL 3000+**M3**	93	1.4	−50	34	114	4.0	15
SMP7	PCL 4000+**M1**	104	1.4	−50	54	76	43	9

[a] Determined by GPC (THF, polystyrene standards).
[b] Determined by DSC (second heating).
[c] Determined by DMTA.

resistance to deformation at low temperatures while elastic recovery should be facilitated at $T > T_{ms}$. Although **SMP7** had by far the largest E'_c/E'_r in the series, the polymer possessed an insufficient concentration of hard segments and lacked the essential rubbery plateau. Both the low T_{ms} and the low modulus above T_{ms} for **SMP7** were attributed to dilution of the hard segment, as well as to a reduction in crystallinity of the hard segment that occurred with increasing soft segment length.

DMTA measurements give also an estimate of the flow temperature (T_{flow}) at which the storage modulus falls below 1 MPa. The flow temperature is important from an application point of view since it provides an upper temperature limit above, which the polymer will deform irreversibly. For the polymers shown in Fig. 8(a), T_{flow} decreased steadily with increasing length of the soft segment length: PCL 2000 (137 °C, **SMP1**) > PCL 3000 (103 °C, **SMP4**) > PCL 4000 (70 °C, **SMP7**). From this, it was readily evident that polymer

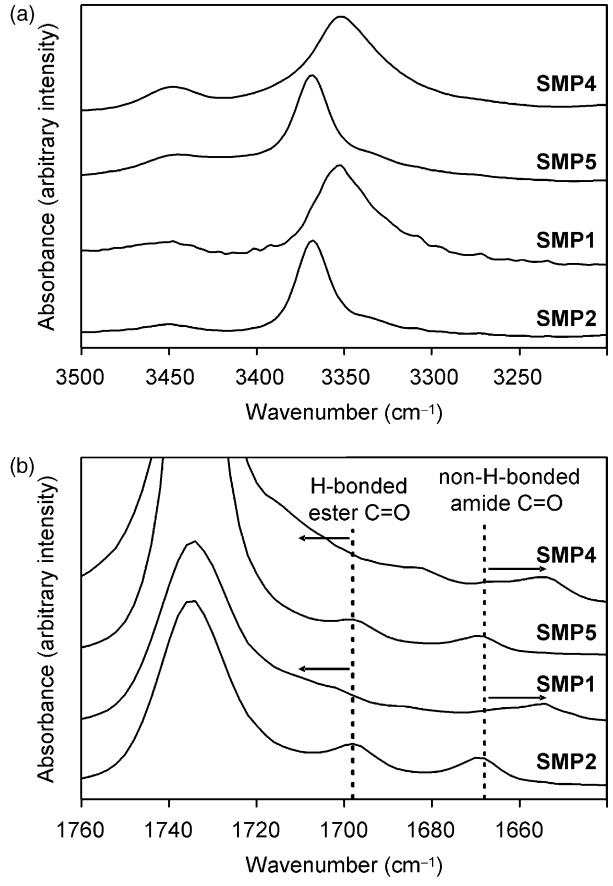

Fig. 7. IR spectra of polymers **SMP1**, **SMP2**, **SMP4**, and **SMP5**: (a) N–H and (b) C=O stretching regions. The arrows indicate in which direction the C=O bands shift in **SMP1** and **SMP4**.

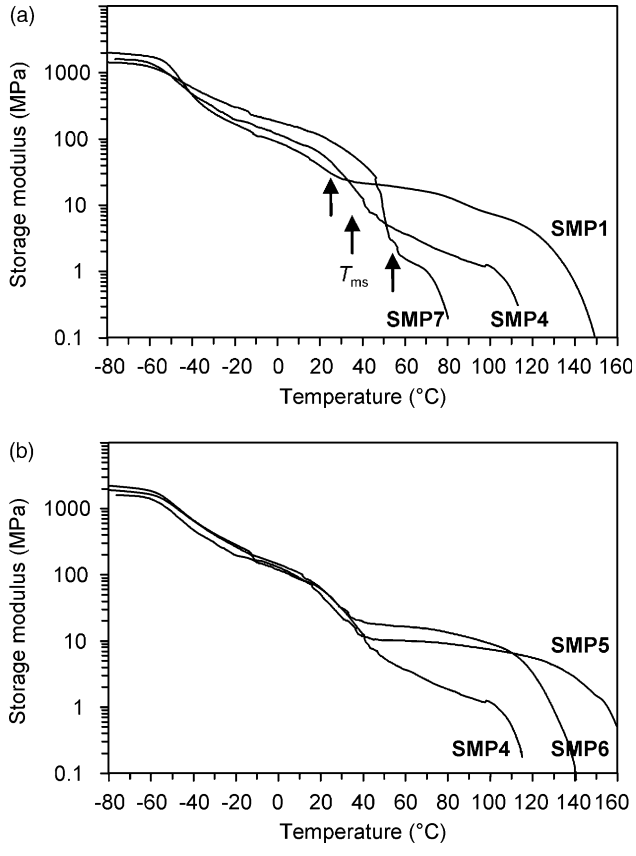

Fig. 8. Plot of the storage modulus as a function of temperature for various SMPs (a) having the same terephthalamide hard segment (arrows indicate T_{ms}, as determined by DSC, for each polymer) or (b) having the same poly(ε-caprolactone) 3000 soft segment.

SMP7 would not be suitable as a shape-memory polymer owing to its low T_{flow}, which was only 15 °C above T_{ms}.

Even though **SMP1–SMP3** possessed extended rubbery plateaus, the elasticity ratios for the three PCL 2000-based polymers were much too low to provide any useful shape-memory effect. Low elasticity ratios indicate poor resistance to deformation below T_{ms} as well as poor recovery above T_{ms}. Fig. 8(b) shows the temperature dependence of the storage modulus for the three polymers containing PCL 3000 soft segments. Again, a rubbery plateau and a flow temperature well above T_{ms} can be identified in each case. The elasticity ratio of **SMP4** was large enough for this polymer to exhibit a thermal shape-memory effect. Naphthalenedicarboxamide units in the hard segment of polymer **SMP5** widened the rubbery plateau to higher temperatures and raised the rubbery modulus. Consequently, this polymer's elasticity ratio was considerably reduced and more on the borderline. The elasticity ratio of **SMP6** was even lower than that of **SMP5**. The biphenyldicarboxamide hard segment had turned out to lead to unsatisfactory elastic behavior in related thermoplastic elastomers, and **SMP6** was not pursued any further [22].

A jump in the tan δ vs. temperature curve has been previously noted in polyurethane SMPs based on PCL 4000 or PCL 8000 [16]. Fig. 9 shows that neither **SMP4** nor **SMP5** gave rise to any sudden rise in tan δ at T_{ms}. The gradual increase in tan δ above T_{ms} for **SMP4** suggested that, above about 70 °C, this polymer might be susceptible to some damping and irreversible deformation. **SMP5** possessed instead an extended plateau between room temperature and about 120 °C, which was due to both storage (Fig. 8) and loss modulus (Fig. 9(a)) remaining almost unchanged over this wide temperature range. All in all, the DMTA measurements indicated that **SMP4**, and to some extent **SMP5**, should exhibit useful shape-memory properties.

3.6. Tensile tests and shape-memory effect

On the basis of the DMTA results, polymers **SMP4** and **SMP5** were selected for extended tensile testing. Both polymers possessed elongations at break of around 800%. Shape-memory properties were quantified by repeatedly straining cast films to $\varepsilon_m = 200$, 300, or 400% at room temperature (19 °C), when soft segments were still partially crystalline. Immediately after that, the samples were allowed to relax at room temperature and then heated to 55 °C (above T_{ms}) for 15 min. Fig. 10(a) depicts the stress–strain curves for five consecutive thermomechanical cycles for a cast film of **SMP4**. Stretching the polymer film for the first time gave rise to a yield point. Apparently, while there was some resistance during the first cycle, reorientation of the polymer chains in the original cast films facilitated stretching and relaxation from the second cycle onwards [16]. Subsequent cycles showed the typical S-shaped stress–strain curve reminiscent of an elastic material, with the stress values being also considerably reduced at the same time. Although cyclic hardening is common in polyurethane-based SMPs, it was not observed for **SMP4** [30]. Two initial 'training' cycles, more when strains exceeded

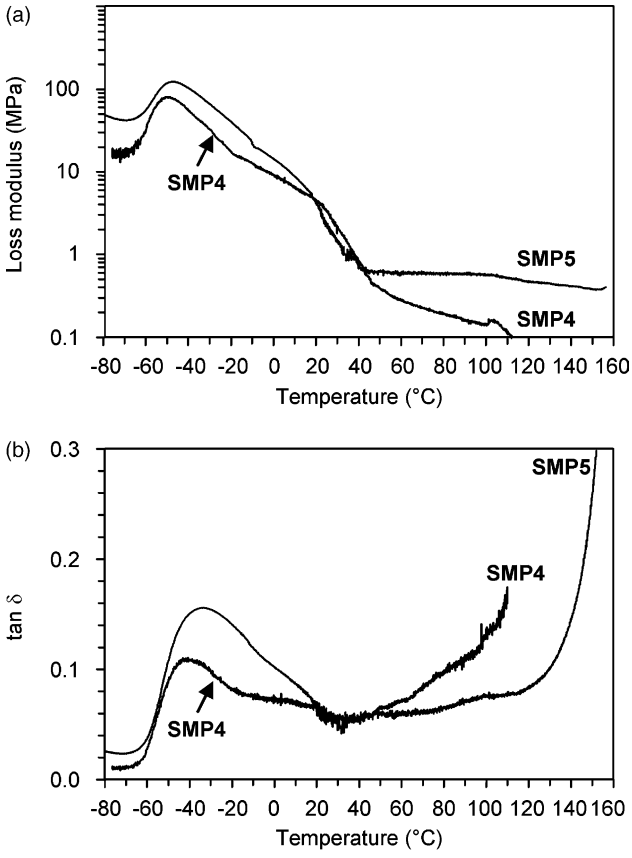

Fig. 9. Plot of (a) loss modulus and (b) tan δ vs. temperature for shape-memory polymers **SMP4** and **SMP5**.

300%, were necessary until the cyclic curves became virtually superimposable. All subsequent cyclic stress–strain curves started almost at the same strain value, ε_p, to which they returned again as the temporarily deformed samples were heated to 55 °C. This behavior can be exploited in order to obtain uniform cyclic deformation, by simply subjecting the material to several extension–relaxation cycles prior to practical use.

Fig. 11 confirms that, from the third cycle onwards, polymer **SMP4** gave rise to high strain recovery rates (up to 99%) that were more or less independent of whether the films were stretched to 200, 300, or 400%. Strain recovery values tended to be about 90% on average as long as ε_m remained limited to 200 or 300%, whereas strain recovery declined progressively with the number of cycles when ε_m was raised to 400%. Except for the cyclic tests at 200% elongation, strain fixity averaged around 78%. The optimum strain value at which polymer **SMP4** displayed both good strain recovery and acceptable strain fixity was 300%. Strain recovery generally deteriorated at a higher ε_m value, whereas a small ε_m tended to affect strain fixity.

Polymer **SMP5** possessed a higher rubbery modulus than **SMP4**, and higher stresses were necessary to stretch the sample (Fig. 10(b)). The higher modulus of **SMP5** points towards a higher degree of crystallinity for its hard segment and was evident from stronger T_{mh} melting endotherms in the DSC. The

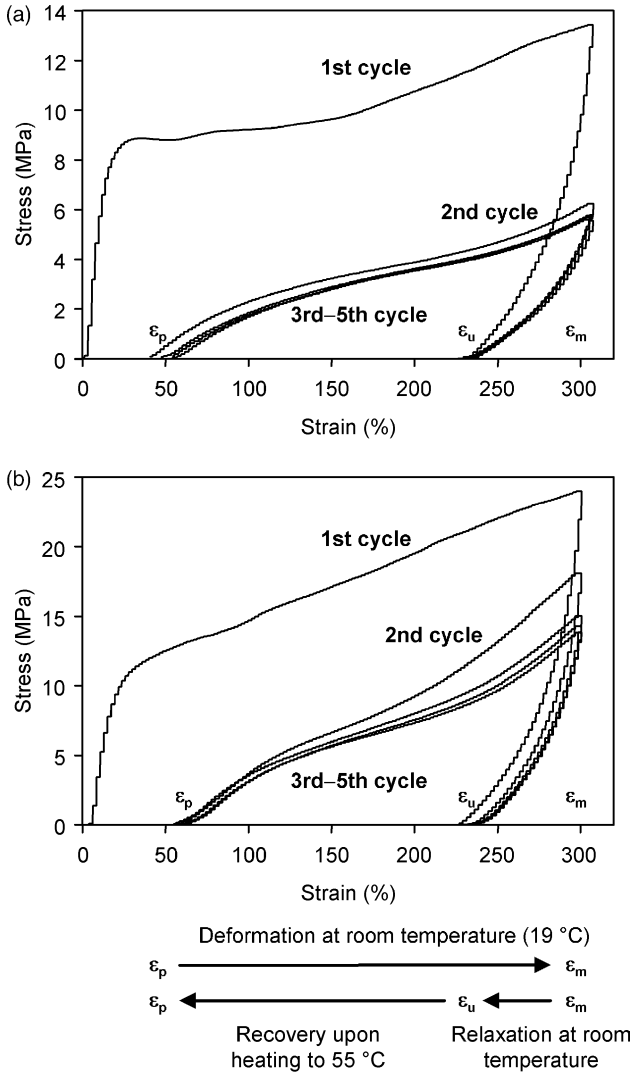

Fig. 10. Cyclic thermomechanical test of a cast film of (a) **SMP4** and (b) **SMP5**. At the beginning of each cycle, the sample was strained to $\varepsilon_m = 300\%$ at room temperature (19 °C) at a speed of 50 mm min^{-1}. Some strain was recovered upon unloading at room temperature, thus reducing the strain value to ε_u. The sample was then heated to 55 °C for 15 min. At this point, a strain ε_p was reached. Cooling to 19 °C finished one cyclic test. The next cycle started again from ε_p and at room temperature.

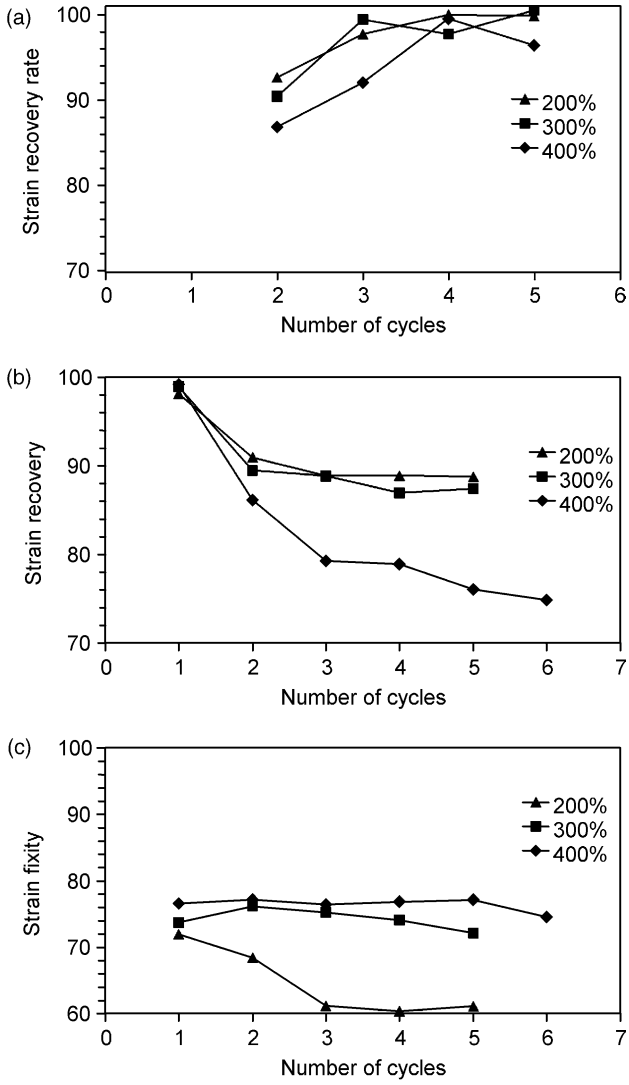

Fig. 11. Strain recovery rate, strain recovery and strain fixity for **SMP4** as a function of the number of cycles.

observation that repeat cycles were no longer superimposed was most likely due to an increase in the stiffness of the polymer requiring more training cycles to reach optimum orientation of the three-dimensional hard segment domains towards the one-dimensional external strain. Despite this, recovery was still surprisingly good, although it worsened slightly as both the number of cycles and ε_m increased. On the other hand, shape fixity remained almost constant even after seven cycles. The optimum ε_m value for obtaining the best shape-memory properties was once again 300%, for which a strain recovery rate of 99.5% and a strain fixity of 79% could be observed.

Both **SMP4** and **SMP5** displayed excellent strain recovery rates comparable to some of the best polyurethane systems [17]. However, strain fixity remained lower, with an average of around 78%, which was primarily a consequence of the cold-drawing process and the straining speed of 50 mm min^{-1} used in this paper. It should be noted that the high strain fixity values reported in the literature were usually obtained by elongating samples much more slowly and at a temperature above T_{ms}, then allowing the chains to relax for at least 5 min, before finally fixing the temporary shape by cooling to −20 °C [8,17]. While such a process may give better strain fixity values, it has the disadvantage that an extra heating–cooling step and more time is needed; in addition, considerable care has to be taken not to break a sample when elongations are carried out at elevated temperature.

It is important to note that the related polyurethane-based SMPs required a much higher weight fraction of hard segment blocks (up to 45%) for optimum performance [16,17]. In contrast, **SMP4** and **SMP5** showed a highly promising performance even though these polymers possessed a very low concentration of hard segments of about 12 wt% as well as comparatively short PCL 3000 soft segments, which are considered unsuitable in the case of polyurethane SMPs [31].

4. Conclusions

Thermoplastic shape-memory polymers with short aramid hard segments and PCL 2000, 3000 and 4000 soft segments are reported for the first time in this paper. The polymers were obtained by a low-temperature solution polymerization. Aramid units gave high elongations at break (800%) similar to many of their polyurethane counterparts. More importantly, they provided effective physical cross-links even at a relatively low hard segment content of about 12 wt%. While the modulus–temperature curves determined by DMTA measurements were typical for thermoplastic elastomers, recovery after elongation at room temperature remained poor.

Two aramid-containing polymers, **SMP4** and **SMP5** (both derived from PCL 3000), possessed promising characteristics of shape-memory polymers. Their dynamic properties showed a drop in modulus at around T_{ms} that was followed by an extended rubbery plateau. The elasticity ratio $E'_c/E'_r > 4$ served as a guideline as it indicated a sufficient drop in modulus between the room temperature value (E'_c), when the soft segment was partially crystalline, and the modulus at the onset of the rubbery region (E'_r). The modulus at room temperature was sufficiently low to ensure that polymer films could be readily deformed by cold-drawing, which is less complicated as the procedure reported for most shape-memory polymers so far, where programming is performed at a temperature above the thermally induced shape-memory transition. After an initial 'training' cycle, both SMPs showed S-shaped stress–strain characteristics reminiscent of elastomers, although recovery of the original shape and length required a brief heat treatment to 55 °C. Stress–strain curves became almost superimposable from the third cycle onwards. Although the cold-drawing process is not a unique feature of this class of SMPs, our two polymers turned out to be ideally suited for loading at room temperature (cold-drawing), which has an important economical advantage as it avoids the need for an extra heating–cooling step to achieve the temporary shape. The observed shape-memory effect could find applications in actuators, toys and simple heat-sensitive devices. Shape-memory polymers with aramid hard segments, with their good mechanical strength and promising cold-drawing performance, offer indeed an alternative to polyurethane-based SMPs.

Acknowledgements

We thank EPSRC for a project studentship, Solvay Caprolactones/Brian Jones and Associates Ltd for a gift of various poly(ε-caprolactone)-diols, Ms K. Müller for the preparation of **SMP7**, and Dr I. J. McEwen for helpful discussions.

References

[1] Wei ZG, Sandström R, Miyazaki S. J Mater Sci 1998;33:3743–62.
[2] Maitland DJ, Lee AP, Schumann DL, Silva LD, University of California. US Patent No. 6102917; 2000.
[3] Duerig T, Pelton A, Stockel D. Mater Sci Eng 1999;A273–275:149–60.
[4] Lendlein A, Kelch S. Angew Chem Int Ed 2002;41:2034–57.
[5] Liu C, Chun SB, Mather PT, Zheng L, Haley EH, Coughlin EB. Macromolecules 2002;35:9868–74.
[6] Rousseau IA, Mather PT. J Am Chem Soc 2003;125:15300–1.
[7] Liu G, Ding X, Cao Y, Zheng Z, Peng Y. Macromolecules 2004;37:2228–32.
[8] Lendlein A, Schmidt AM, Langer R. Proc Natl Acad Sci USA 2001;98:842–7.
[9] Kobayashi K, Hayashi S, Mitsubishi Jukogyo Kabushiki Kaisha. US Patent No. 5128197; 1992.
[10] Hayashi S, Wakita Y, Mitsubishi Jukogyo Kabushiki Kaisha. US Patent No. 5135786; 1992.
[11] Tobushi H, Hara H, Yamada E, Hayashi S. Smart Mater Struct 1996;5:483–91.
[12] Alteheld A, Feng Y, Kelch S, Lendlein A. Angew Chem Int Ed 2005;44:1188–92.
[13] Kim BK, Shin YJ, Cho SM, Jeong HM. J Polym Sci, Part B: Polym Phys 2000;38:2652–7.
[14] Tobushi H, Hashimoto T, Ito N, Hayashi S, Yamada E. J Intell Mater Syst Struct 2001;12:283–7.
[15] Li FK, Zhang X, Hou JN, Xu M, Lu XL, Ma DZ, et al. J Appl Polym Sci 1997;64:1511–6.
[16] Kim BK, Lee SY, Xu M. Polymer 1996;37:5781–93.
[17] Lendlein A, Langer R. Science 2002;296:1673–6.
[18] Niesten MCEJ, Feijen J, Gaymans RJ. Polymer 2000;41:8487–500.
[19] Niesten MCEJ, Harkema S, van der Heide E, Gaymans RJ. Polymer 2001;42:1131–42.
[20] Niesten MCEJ, ten Brinke JW, Gaymans RJ. Polymer 2001;42:1461–9.
[21] Niesten MCEJ, Gaymans RJ. J Appl Polym Sci 2001;81:1372–81.
[22] Rabani G, Rosair GM, Kraft A. J Polym Sci, Part A: Polym Chem 2004;42:1449–60.
[23] Kraft A, Rabani G. Polym Mater Sci Eng 2004;90:41–2.
[24] Luftmann H, Rabani G, Kraft A. Macromolecules 2003;36:6316–24.
[25] Oishi Y, Kakimoto M, Imai Y. Macromolecules 1988;21:547–50.
[26] Lozano AE, de Abajo J, de la Campa JG. Macromolecules 1997;30:2507–8.
[27] Kubu Y, Yamakawa H, Kirikihira I, Shimosato S, Tosoh Corp. US Patent No. 5760143; 1998.
[28] Rabani G, Luftmann H, Kraft A. Polymer 2005;46:27–35.
[29] Flory PJ. Trans Faraday Soc 1955;51:848–56.
[30] Kim BK, Lee SY, Lee JS, Baek SH, Choi YJ, Lee JO, et al. Polymer 1998;39:2803–8.
[31] Li F, Hou J, Zhu W, Zhang X, Xu M, Luo X, et al. J Appl Polym Sci 1996;62:631–8.